Elastic and absorption cross sections for electron−nitrous oxide collisions

M.-T. Lee and I. Iga

Departamento de Química, UFSCar, 13565-905 São Carlos, São Paulo, Brazil

M. G. P. Homem and L. E. Machado

Departamento de Física, UFSCar, 13565-905 São Carlos, São Paulo, Brazil

L. M. Brescansin

Instituto de Física "Gleb Wataghin," UNICAMP, 13083-970 Campinas, São Paulo, Brazil

In this work, we present a joint theoretical-experimental study on electron-N_2O collisions in the intermediate energy range. More specifically, calculated and measured elastic differential, integral, and momentum-transfer cross sections, as well as calculated total and absorption cross sections are reported. The measurements were performed using a crossed electron-beam–molecular-beam geometry. The angular distribution of the scattered electrons was converted to absolute cross sections using the relative-flow technique. Theoretically, a complex optical potential is used to represent the electron-molecule interaction dynamics in the present calculation. The Schwinger variational iterative method combined with the distorted-wave approximation is used to solve the scattering equations. The comparison of the present calculated results with the measured results as well as with the existing experimental and theoretical data shows good agreement.

I. INTRODUCTION

Electron-N_2O collisions play an important role in a number of physical and chemical processes. For instance, N_2O was found to be important in the chemistry of the upper atmosphere, where it may participate in part of the mechanism of destruction of the ozone layer [1–3]. Also, N_2O lasers have been used as a secondary standard in areas of spectroscopy within the 10-μm region where the frequency of the CO_2 lasers is inadequate [4]. From the academic point of view, N_2O is isoelectronic with CO_2 and both molecules are linear in their ground state. Although it is expected that the similarity of the electronic configurations can lead to similar electron-scattering cross sections, the presence of a moderate dipole moment in N_2O can lead to different forward-scattering behaviors of these two molecules.

In the past two decades, several experimental studies on e^--N_2O scattering were reported in the literature. Grand total (elastic + inelastic) cross section (TCSs) measurements were performed by Kwan *et al.* [5] and Szmytkowski *et al.* [6,7]. Experimental elastic differential cross sections (DCS's) have also been reported by several authors [8–11]. Vibrational excitation DCS's for incident energies in the (2–8)-eV region were reported by Azria *et al.* [12], Tronc *et al.* [13], and Andrić and Hall [14]. Recently, Barnett *et al.* [15] have reported an observation of metastable N_2 and O from electron-impact dissociative excitation of N_2O. Differential inelastic e^--N_2O scattering cross sections for the excitation to the $^1\Pi$ and $2\,^1\Sigma^+$ states were reported by Marinković *et al.* [9]. Electron-impact ionization cross sections of this molecule were also measured by Iga *et al.* [16]. Very recently, elastic and vibrational excitation DCS's for e^--N_2O collisions were reported by Kitajima *et al.* [17,18].

On the theoretical side, low-energy elastic e^--N_2O collisions have been the subject of several recent investigations,

both at the static-exchange (SE) [19–21] and/or static-exchange-polarization (SEP) levels of approximation [20,22,23]. Despite that, most of these studies were performed at incident energies below 80 eV. Above this energy, both theoretical and experimental investigations are scarce. To our knowledge, there is only one measurement [10] of e^--N_2O scattering cross sections and no theoretical studies reported in the literature. Considering the importance of this molecule in various areas of application, the knowledge of several cross sections for e^--N_2O interaction in the intermediate energy range (from ionization threshold to a few 100 eV) will certainly be very important for plasma modeling and atmospheric and planetary studies. Also, it is well known that the absorption effects play an important role on e^--molecule scattering in this energy range. Although the main features of these effects are known, taking them into account in an *ab initio* treatment is a very difficult task. Therefore, the use of model absorption potentials seems to be presently the only practical manner for studying e^--atom and e^--molecule collisions. Recently, the validity of several model absorption potentials was investigated in the calculations of elastic DCS's and TCS's for e^--CH_4 scattering in the intermediate energy range [24]. A modified version of the free-electron gas (FEG) of Staszewska *et al.* [25] was found to better reproduce the experimental results. Although the extension of this simple model potential to general e^--molecule scattering calculations is clearly of interest, its validity for electron scattering by other molecular targets needs to be investigated.

In this work, we report a joint theoretical and experimental study on electron scattering by N_2O in the intermediate energy range. More specifically, calculated TCS's and elastic DCS's, integral cross sections (ICS's), and momentum-transfer cross sections (MTCS's) for electron-impact energies ranging from 20 to 800 eV, as well as measured elastic

cross sections (DCS's, ICS's, and MTCS's) in the (50–800)-eV range are presented. A complex optical potential is used to represent the e^--N$_2$O interaction dynamics, while a combination of the Schwinger variational iterative method (SVIM) [26] and the distorted-wave approximation (DWA) [27–29] is used to solve the scattering equations. Although the present study is unable to provide directly the electron-impact total ionization cross sections (TICS's) for N$_2$O, the difference between the calculated TCS's and ICS's provides an estimate of the total absorption cross sections (TACS's), which account for all inelastic contributions including both excitation and ionization processes. Nevertheless, Joshipura *et al.* [30] have observed that for a set of molecules, the ionization dominates the inelastic processes, the values of the TICS's being about 80% of the TACS's at energies around 100 eV and about 100% for energies above 300 eV. Therefore, a comparison of the present calculated TACS's with experimental and calculated TICS's is meaningful and would provide insights of the electron-impact ionization dynamics of this molecule. Experimentally, intensities of scattered electrons were measured in the 15°–130° angular range. These intensities were converted to absolute cross sections by using the relative-flow technique.

The organization of this paper is as follows. In Sec. II, we describe briefly the theory used and also give some details of the calculation. In Sec. III, some experimental details are briefly described. Finally, in Sec. IV we compare our calculated results with the present experimental and other theoretical and experimental data available in the literature.

II. THEORY AND CALCULATION

Since the details of the SVIM and the DWA have already been presented in previous works [26–29], only a brief outline of the theory will be given here. Within the adiabatic-nuclei-rotation framework, the DCS's for the excitation from an initial rotational level j_0 to a final level j are given by

$$\frac{d\sigma}{d\Omega}(j \leftarrow j_0) = \frac{k_j}{k_0} \frac{1}{(2j_0+1)} \sum_{m_j m_{j_0}} |\langle jm_j|f|j_0 m_{j_0}\rangle|^2, \quad (1)$$

where j_0, m_{j_0} (j, m_j) are the rotational quantum numbers of the initial (final) rotational state, f is the laboratory-frame (LF) electronic part of the scattering amplitude, and k_0 and k_j are the linear momentum magnitudes of the incident and scattered electron, respectively. Using the rigid-rotor approximation, the wave function for a given $|jm_j\rangle$ is

$$|jm_j\rangle = \left[\frac{(2j+1)}{8\pi^2}\right]^{1/2} D_{m_j 0}^j(\hat{R}), \quad (2)$$

where $D_{m_j 0}^j$ are the usual finite rotational matrix elements.

The partial-wave expansion of the rotational excitation scattering amplitude is given by

$$\langle jm_j|f|j_0 m_{j_0}\rangle = 4\pi[(2j+1)(2j_0+1)]^{1/2}$$

$$\times \sum_{ll'm} (-1)^{m+m_{j_0}+1} i^{l-l'} T_{ll'm} Y_{l'm_j-m_{j_0}}$$

$$\times \sum_L (2L+1)^{-1} (l0l'm_j-m_{j_0}|$$

$$\times ll'Lm_j-m_{j_0})(l-ml'm|ll'L0)$$

$$\times (j-m_j j_0 m_{j_0}|jj_0 Lm_{j_0}-m_j)$$

$$\times (j0j_0 0|jj_0 L0), \quad (3)$$

where $T_{ll'm}$ are the scattering T-matrix elements, Y_{lm} are the usual spherical harmonics, and $(l_1 m_1 l_2 m_2|l_1 l_2 l_3 m_3)$ are Clebsch-Gordan coefficients.

In order to compare our data with the rotationally unresolved experimental DCS's for elastic e^--molecule scattering, we calculate rotationally summed DCS's as

$$\frac{d\sigma}{d\Omega} = \sum_{j=0} \frac{d\sigma}{d\Omega}(j \leftarrow j_0). \quad (4)$$

In the present study, the e^--molecule scattering dynamics is represented by a complex optical potential, given by

$$V_{opt}(\vec{r}) = V^{SEP}(\vec{r}) + iV_{ab}(\vec{r}), \quad (5)$$

where V^{SEP} is the real part of the interaction potential formed by static (V_{st}), exchange (V_{ex}), and correlation-polarization (V_{cp}) contributions, whereas V_{ab} is an absorption potential. V_{st} and V_{ex} are obtained exactly from a Hartree-Fock self-consistent field (SCF) target wave function. A parameter-free model potential introduced by Padial and Norcross [31] is used to account for the correlation-polarization contributions. In this model, a short-range correlation potential between the scattering and the target electrons is defined in an inner region and a long-range polarization potential is defined in an outer region. The first crossing of the correlation and polarization potential curves defines the inner and the outer regions. The correlation potential is calculated by a FEG model, derived from the target electronic density, according to Eq. (9) of Padial and Norcross [31]. In addition, the asymptotic form of the polarization potential is used for the long-range electron-target interaction. The dipole polarizabilities $\alpha_0 = 20.22$ a.u. and $\alpha_2 = 13.17$ a.u. [32] were used to calculate the asymptotic form of V_{cp}. No cutoff or other adjustable parameters are needed for the calculation of V_{cp}.

The absorption potential V_{ab} in Eq. (5) is given as

$$V_{ab}(\vec{r}) = -\rho(\vec{r})(T_L/2)^{1/2}(8\pi/5k^2 k_F^3)H(\alpha+\beta-k_F^2)$$

$$\times (A+B+C), \quad (6)$$

where

$$T_L = k^2 - V^{SEP}, \quad (7)$$

$$A = 5k_F^3/(\alpha - k_F^2), \tag{8}$$

$$B = -k_F^3[5(k^2 - \beta) + 2k_F^2]/(k^2 - \beta)^2, \tag{9}$$

and

$$C = 2H(\alpha + \beta - k^2)\frac{(\alpha + \beta - k^2)^{5/2}}{(k^2 - \beta)^2}. \tag{10}$$

In Eqs. (6)–(10), k^2 is the energy (in rydbergs) of the incident electron, k_F is the Fermi momentum, and $\rho(\vec{r})$ is the local electronic density of the target. $H(x)$ is a Heaviside function defined by $H(x)=1$ for $x \geq 0$ and $H(x)=0$ for $x < 0$. According to Staszewska et al. [25],

$$\alpha(\vec{r},E) = k_F^2 + 2(2\Delta - I) - V^{SEP} \tag{11}$$

and

$$\beta(\vec{r},E) = k_F^2 + 2(I - \Delta) - V^{SEP}, \tag{12}$$

where Δ is the average excitation energy and I is the ionization potential.

The Lippmann-Schwinger scattering equation for elastic $e^- $-$N_2O$ collisions is solved using the SVIM, considering only the real part of the optical potential. In SVIM calculations, the continuum wave functions are single-center expanded as

$$\chi_{\vec{k}}^{\pm}(\vec{r}) = \left[\frac{2}{\pi}\right]^{1/2} \sum_{lm} \frac{(i)^l}{k} \chi_{klm}^{\pm}(\vec{r}) Y_{lm}(\hat{k}), \tag{13}$$

where the superscripts $+$ and $-$ denote the incoming-wave and outgoing-wave boundary conditions, respectively. The absorption part of the T matrix is calculated via the DWA as

$$T_{abs} = i\langle \chi_f^- | V_{ab} | \chi_i^+ \rangle. \tag{14}$$

In addition, the TCS's are calculated by using the optical theorem [33].

In this study, a standard $[10s5p/4s3p]$ basis set of Dunning [34] augmented by one s ($\alpha = 0.028$), one p ($\alpha = 0.025$), and one d ($\alpha = 0.8$) uncontracted functions for nitrogen atom and three s ($\alpha = 0.05, 0.02$, and 0.005), one p ($\alpha = 0.04$), and three d ($\alpha = 1.7, 0.85$, and 0.34) functions for oxygen atom is used for the calculation of the SCF target wave function. At the experimental equilibrium geometry of the ground-state N_2O ($R_{N-N} = 2.127$ a.u., $R_{N-O} = 2.242$ a.u.), this basis set yielded a calculated SCF energy of $-183.723\,896$ a.u. and a dipole moment of $0.648\,11$ D, to be compared with the near-Hartree-Fock values of $-183.773\,825$ a.u. and 0.6585 D [23], respectively. However, it should be noted that the experimental value of the dipole moment, 0.1609 D [35], is much smaller than the calculated Hartree-Fock value.

In the present study, we have limited the partial-wave expansion of the continuum wave functions as well as of the T-matrix elements up to $l_{max} = 30$ and $m_{max} = 17$. Since N_2O is a polar molecule, these partial-wave expansions converge
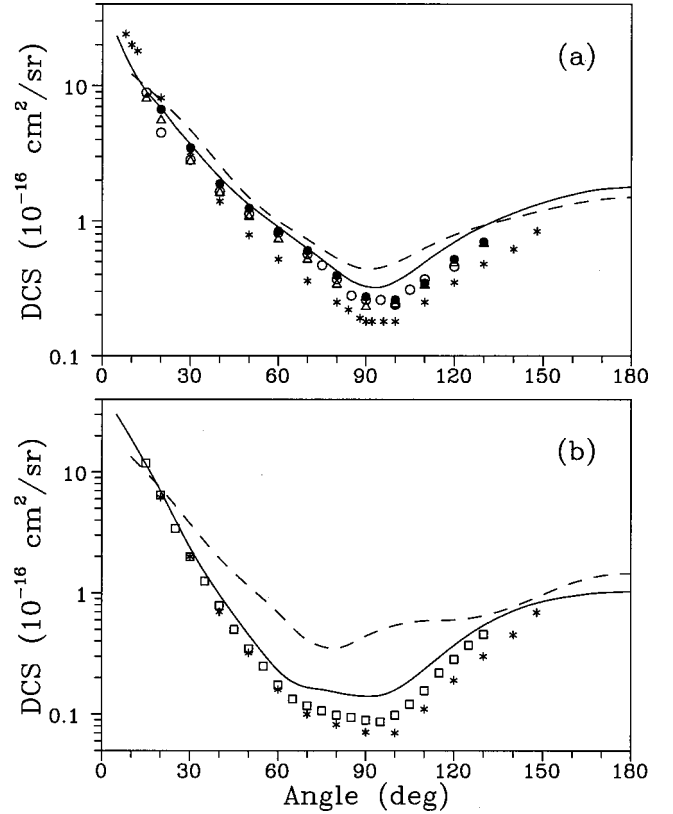

FIG. 1. DCS's for elastic e^--N_2O scattering at (a) 20 eV and (b) 50 eV. Full curve, present rotationally summed results; dashed line, calculated results of Michelin et al. [19]; open squares, present experimental data; full circles, experimental data of Kitajima et al. (SU group) [18]; open triangles, experimental data of Kitajima et al. (ANU group) [18]; open circles, experimental data of Johnstone and Newell [11]; stars, experimental data of Marinković et al. [9].

slowly due to the long-range dipole interaction potential. Therefore, a Born-closure formula is used to account for the contribution of higher partial-wave components to the scattering amplitudes. Accordingly, Eq. (3) is rewritten as

$$\langle jm_j | f | j_0 m_{j_0} \rangle$$

$$= 4\pi[(2j+1)(2j_0+1)]^{1/2} \sum_{ll'm} (-1)^{m+m_{j_0}+1}$$

$$\times i^{l-l'}(T_{ll'm} - T_{ll'm}^{Born}) Y_{l'm_j - m_{j_0}} \sum_L (2L+1)^{-1}$$

$$\times (l0l'm_j - m_{j_0} | ll'Lm_j - m_{j_0})(l-ml'm | ll'L0)$$

$$\times (j-m_j j_0 m_{j_0} | jj_0 Lm_{j_0} - m_j)(j0j_0 0 | jj_0 L0)$$

$$+ \langle jm_j | f^{Born} | j_0 m_{j_0} \rangle, \tag{15}$$

where $T_{ll'm}^{Born}$ are the partial-wave expanded T-matrix elements. They are calculated using the first Born approximation. For a rotating dipole, they are given by
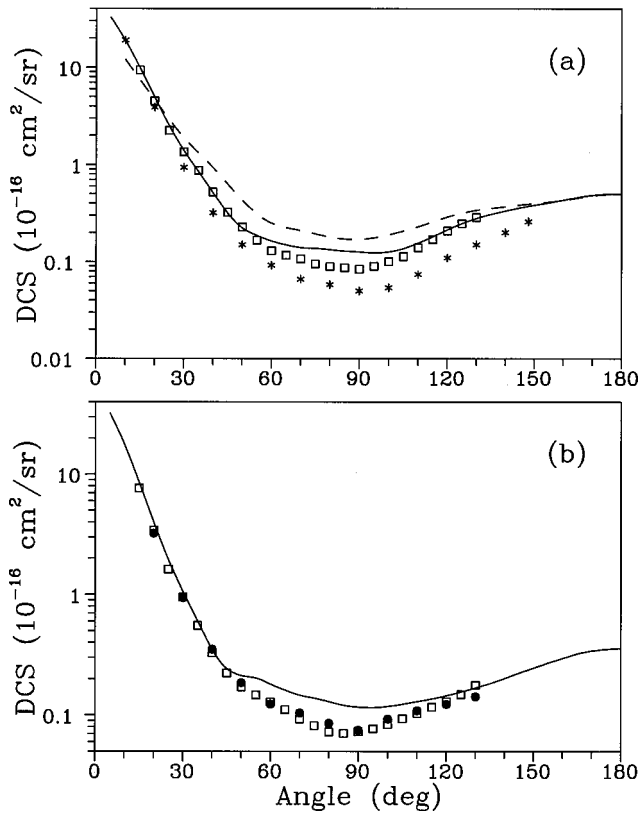
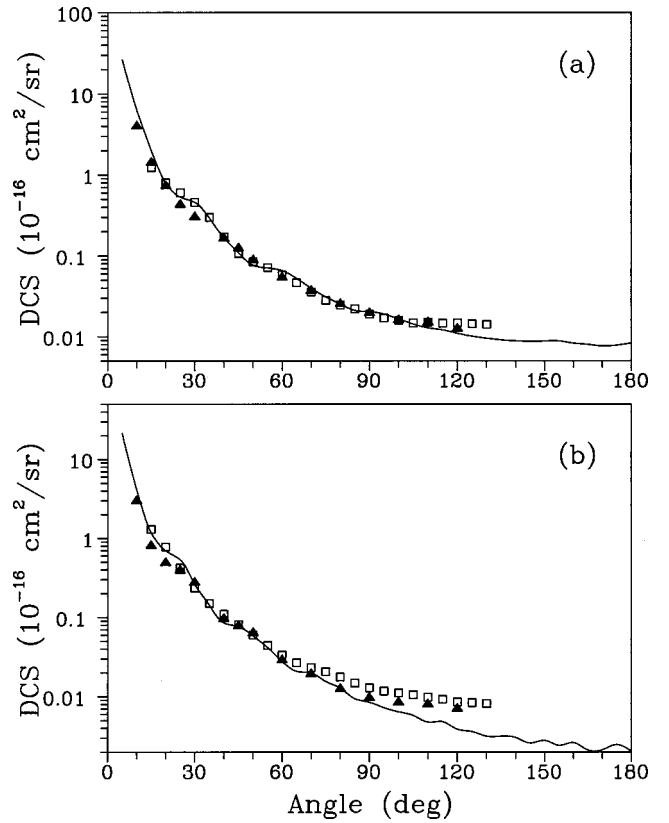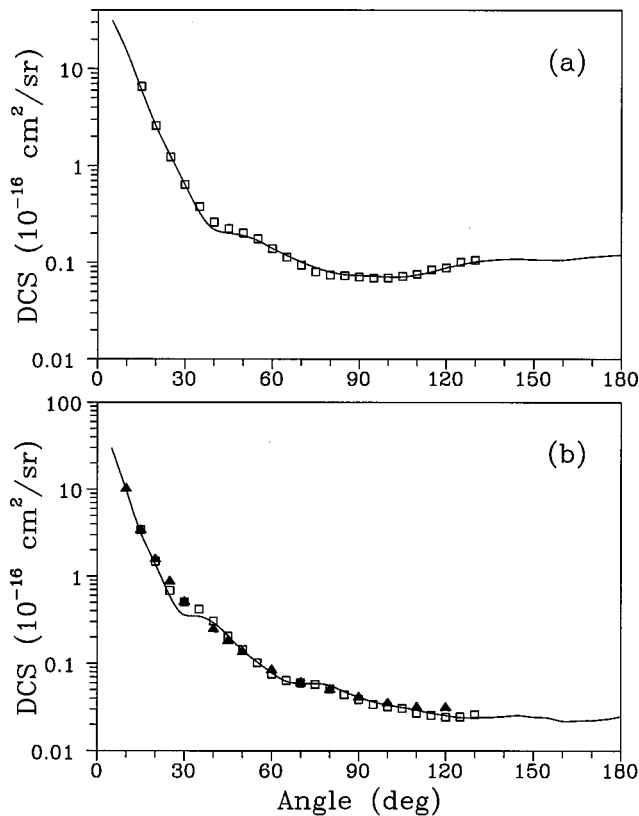FIG. 2. Same as Fig. 1 but for (a) 80 eV and (b) 100 eV.

FIG. 4. Same as Fig. 3 but for (a) 500 eV and (b) 800 eV.

FIG. 3. Same as Fig. 1 but for (a) 150 eV and (b) 300 eV. Full triangles, experimental results of Nogueira *et al.* [10].

$$T_{ll'm}^{Born} = - \frac{D}{L} \left[\frac{(L+m)(L-m)}{(2L+1)(2L-1)} \right]^{1/2}, \qquad (16)$$

where $L=l'$ when $l'=l+1$ and $L=l$ when $l'=l-1$. In addition, for $j_0=0$, the full LF Born electron-scattering amplitude for a rotating dipole with dipole moment D is given by

$$f^{Born} = \frac{2D}{q} \left[\frac{4\pi}{3} \right]^{1/2} i \sum_m D_{m0}^1(\hat{R}) Y_{1m}(\hat{q}'), \qquad (17)$$

where $\vec{q}' = \vec{k}_0' - \vec{k}_f'$ is the momentum transferred during the collision. Further, rotationally summed cross sections are obtained by summing up the contributions of individual rotational excitation cross sections. Sufficient rotational states were included to ensure the convergence to be within 0.2%.

III. EXPERIMENT

Details of our experimental setup and procedure have already been presented elsewhere [36,37]. Basically, a crossed electron-beam–molecular-beam geometry is applied to measure the relative intensity of the scattered electrons as a function of the scattering angles.

The electron gun used is composed by a hairpin tungsten filament, a triode extraction, a set of einzel lenses, and two sets of electrostatic deflectors, which allow better positioning of the electron beam in the interaction region. The electron beam with an estimated diameter of 1 mm is generated with-
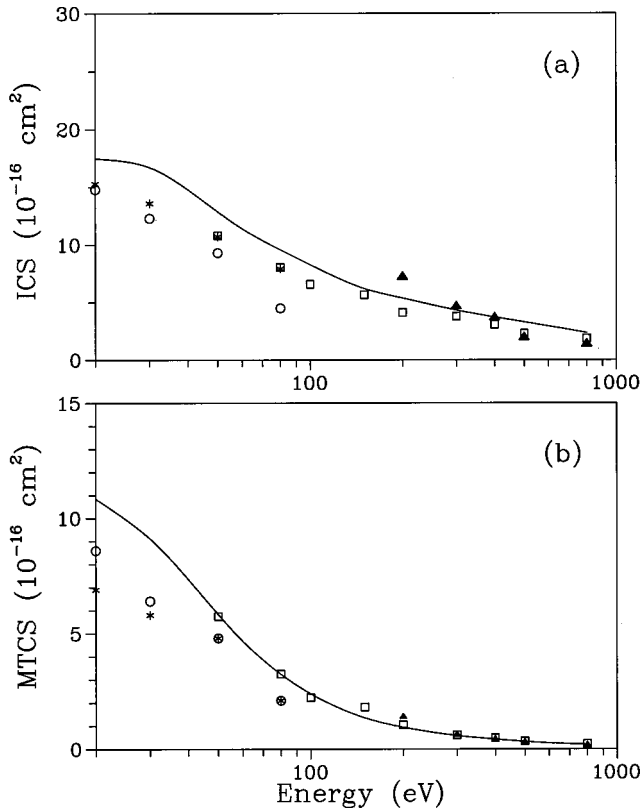
FIG. 5. (a) ICS's and (b) MTCS's for elastic electron scattering by N_2O in the (20–800)-eV range. The symbols are the same as in Fig. 3.
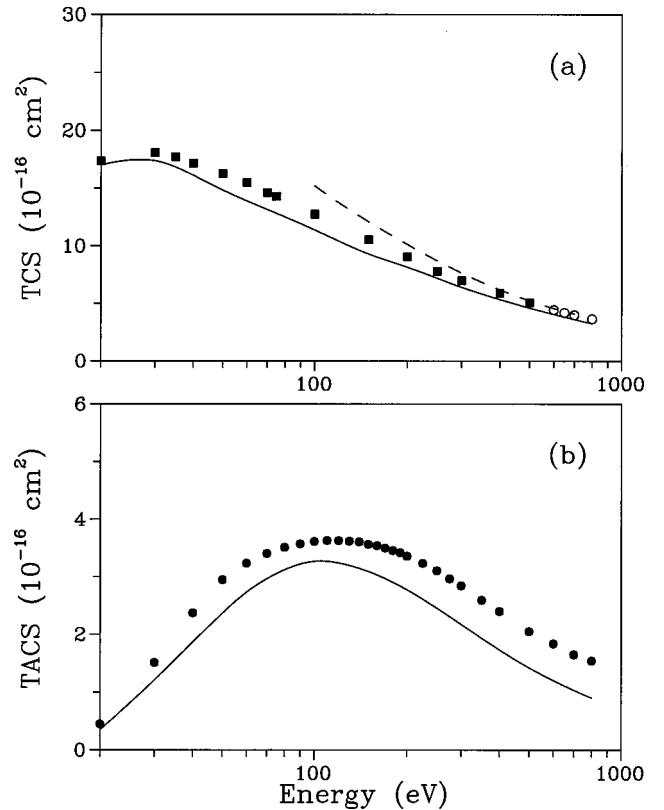

FIG. 6. (a) TCS's and (b) TACS's for electron scattering by N_2O in the (20–800)-eV range. Full curve, present calculated results; dashed line, results of Joshipura and Patel [55] calculated using the additivity rule; full squares, experimental TCS's of Kwan et al. [5]; open circles, experimental TCS's of Xing et al. [54]; full circles, experimental ionization cross sections of Iga et al. [16].

out prior energy selection. The typical beam current is ≈ 100 nA in the covered energy range. A molecular beam flows into the vacuum chamber via a capillary array. This array has a length $L = 5$ mm with individual capillary diameter $D = 0.05$ mm and an aspect ratio $\gamma = D/L = 0.01$. The scattered electrons are energy filtered by a retarding-field energy selector with a resolution of about 1.5 eV. Since the lowest excitation threshold of N_2O is 8.2 eV [9], this resolution is sufficient to distinguish electronically inelastic scattered electrons. After being energy-analyzed, the elastically scattered electrons are detected by a channeltron.

During the measurements, the working pressure in the vacuum chamber is around 5×10^{-7} Torr. The recorded scattering intensities are converted into absolute elastic DCS's using the relative-flow technique [38–46]. Accordingly, the DCS's for a gas x under determination can be related to known DCS's of a secondary standard gas std as

$$(DCS)_x = (DCS)_{std} \frac{I_x}{I_{std}} \frac{n_{std}}{n_x} \left(\frac{M_{std}}{M_x} \right)^{1/2}, \quad (18)$$

where I is the scattered electron intensity, n is the flow rate, and M is the molecular weight. The above equation is valid if the density distribution of both gases, x and std, are closely the same. According to Olander and Kruger [47], this requirement is fulfilled under two conditions: the mean free paths λ of both gases behind the capillaries should be equal and the Knudsen number K_L, defined as λ/L, must satisfy

the relation $\gamma \lesssim K_L \lesssim 10$. However, several recent investigations have provided experimental evidences that even in beam flow regimes in which the K_L's are significantly lower than γ, Eq. (18) can still be valid [36,44,46].

In the present study, N_2 is used as the secondary standard. The collisional diameters of N_2 and N_2O are 3.14 Å [48] and 3.27 Å, respectively. The latter was calculated using the van der Waals's constants reported in the Ref. [49]. Thus the theoretical pressure ratio for equal K_L will be $\approx 1:1$. We used the working pressure of 5 Torr for both gases. This corresponds to $\lambda = 13.1$ μm and $K_L = 0.0026$. In addition, the $e^- $-$N_2$ absolute cross sections of Jansen et al. [50] in the (100–500)-eV energy range, those of Dubois and Rudd [51] at 50 and 800 eV, and those of Nickel et al. [52] at 80 eV were used for normalization of our data.

Details of the analysis on experimental uncertainties have also been given elsewhere [36,37]. Briefly, they are estimated as follows. Uncertainties of a random nature, such as the pressure fluctuations, electron-beam current readings, background scattering, etc., are estimated to be less than 2%. These contributions combined with the estimated statistical errors give an overall uncertainty of 4% in the relative DCS's for each gas. Also, the experimental uncertainty associated with the normalization procedure is estimated to be 5.7%. These errors combined with the quoted errors [50–52] in the absolute DCS's of the secondary standard provide an overall

TABLE I. Experimental DCS's, ICS's, and MTCS's (in 10^{-16} cm^2) for elastic e^--N$_2$O scattering. The values in the parentheses denote powers of 10.

Angle (deg)	E_0 (eV)								
	50	80	100	150	200	300	400	500	800
15	1.186(1)	9.386(0)	7.656(0)	6.539(0)	3.631(0)	3.409(0)	2.623(0)	1.237(0)	1.301(0)
20	6.454(0)	4.529(0)	3.414(0)	2.584(0)	1.609(0)	1.487(0)	1.220(0)	8.031(−1)	7.767(−1)
25	3.409(0)	2.244(0)	1.618(0)	1.227(0)	7.946(−1)	6.861(−1)	7.342(−1)	6.039(−1)	4.219(−1)
30	1.984(0)	1.352(0)	9.507(−1)	6.375(−1)	4.480(−1)	5.042(−1)	5.779(−1)	4.593(−1)	2.340(−1)
35	1.255(0)	8.698(−1)	5.519(−1)	3.775(−1)	3.109(−1)	4.188(−1)	4.083(−1)	3.005(−1)	1.503(−1)
40	7.865(−1)	5.221(−1)	3.273(−1)	2.610(−1)	2.661(−1)	3.062(−1)	2.414(−1)	1.718(−1)	1.094(−1)
45	4.994(−1)	3.237(−1)	2.222(−1)	2.239(−1)	2.183(−1)	2.056(−1)	1.532(−1)	1.071(−1)	8.146(−2)
50	3.463(−1)	2.276(−1)	1.711(−1)	2.020(−1)	1.682(−1)	1.440(−1)	1.198(−1)	8.453(−2)	5.985(−2)
55	2.486(−1)	1.662(−1)	1.464(−1)	1.763(−1)	1.293(−1)	1.018(−1)	9.699(−2)	7.148(−2)	4.414(−2)
60	1.746(−1)	1.298(−1)	1.278(−1)	1.391(−1)	9.783(−2)	7.576(−2)	8.243(−2)	5.834(−2)	3.334(−2)
65	1.335(−1)	1.170(−1)	1.107(−1)	1.134(−1)	8.041(−2)	6.381(−2)	7.772(−2)	4.643(−2)	2.667(−2)
70	1.177(−1)	1.071(−1)	9.271(−2)	9.409(−2)	7.032(−2)	5.993(−2)	6.814(−2)	3.580(−2)	2.311(−2)
75	1.696(−1)	9.506(−2)	8.166(−2)	7.997(−2)	5.980(−2)	5.760(−2)	5.161(−2)	2.807(−2)	2.056(−2)
80	9.821(−2)	8.939(−2)	7.251(−2)	7.388(−2)	5.548(−2)	5.146(−2)	4.044(−2)	2.449(−2)	1.763(−2)
85	9.420(−2)	8.639(−2)	7.060(−2)	7.289(−2)	5.558(−2)	4.395(−2)	3.577(−2)	2.205(−2)	1.483(−2)
90	8.923(−2)	8.399(−2)	7.293(−2)	7.052(−2)	5.582(−2)	3.871(−2)	3.051(−2)	1.895(−2)	1.290(−2)
95	8.662(−2)	8.979(−2)	7.692(−2)	6.898(−2)	5.697(−2)	3.389(−2)	2.539(−2)	1.699(−2)	1.175(−2)
100	9.811(−2)	1.005(−1)	8.349(−2)	6.923(−2)	5.677(−2)	3.201(−2)	2.224(−2)	1.587(−2)	1.106(−2)
105	1.209(−1)	1.137(−1)	9.332(−2)	7.204(−2)	5.869(−2)	3.070(−2)	1.979(−2)	1.472(−2)	1.055(−2)
110	1.562(−1)	1.399(−1)	1.033(−1)	7.552(−2)	5.787(−2)	2.712(−2)	1.968(−2)	1.510(−2)	9.840(−3)
115	2.191(−1)	1.699(−1)	1.169(−1)	8.402(−2)	6.080(−2)	2.551(−2)	1.837(−2)	1.465(−2)	9.270(−3)
120	2.832(−1)	2.091(−1)	1.290(−1)	8.822(−2)	6.290(−2)	2.435(−2)	1.778(−2)	1.476(−2)	8.570(−3)
125	3.699(−1)	2.476(−1)	1.481(−1)	1.011(−1)	6.732(−2)	2.455(−2)	1.767(−2)	1.443(−2)	8.390(−3)
130	4.553(−1)	2.878(−1)	1.766(−1)	1.064(−1)	7.289(−2)	2.600(−2)	1.762(−2)	1.416(−2)	8.200(−3)
ICS's	1.080(1)	8.040(0)	6.571(0)	5.661(0)	4.124(0)	3.782(0)	3.072(0)	2.283(0)	1.859(0)
MTCS's	5.737(0)	3.251(0)	2.232(0)	1.818(0)	1.049(0)	6.101(−1)	4.762(−1)	3.346(−1)	2.231(−1)

experimental uncertainty of 12% in our absolute DCS's in the (100–800)-eV energy range and about 20% elsewhere.

For scattering angles $\theta < 15°$ and $\theta > 130°$, the DCS's must be extrapolated in order to obtain the ICS's and MTCS's. The extrapolation was carried out by using a phase-shift fitting procedure according to the prescription of Boesten and Tanaka [53], which is valid for a central potential. The overall errors on ICS's and MTCS's are estimated to be 16% in the (100–800)-eV energy range and 24% elsewhere. This fitting procedure, however, cannot reproduce the sharp peak of the DCS's in the forward direction for a polar molecule, thus leading to a possible large error in the ICS's. Instead of the extrapolated values, if the theoretical DCS's are used for forward and backward angles, an increase of around 8% in the ICS's shown in Table I is observed.

IV. RESULTS AND DISCUSSIONS

In Figs. 1–4 we compare our calculated DCS's (rotationally summed) for elastic e^--N$_2$O scattering in the (20–800)-eV energy range with the present measured data and with some available experimental data [9–11,17,18]. The previous calculated DCS's using the Born-closure Schwinger variational method within the SE approximation of Michelin *et al.* [19] are also shown for comparison. At 50 and 100 eV,

our measured DCS's are in good agreement with those of Marinković *et al.* [9] and Kitajima *et al.* [18], respectively. Nevertheless, the experimental data of Marinković *et al.* are $\approx 20\%$ lower than ours at 80 eV for scattering angles $\geq 30°$. For 300 eV and above, our measured DCS's are also in good agreement with those of Nogueira *et al.* [10].

Comparing our calculated DCS's with experiments, they are in general good agreement with the measured data in the entire energy range covered herein. In general, our calculated results agree better with the experimental data than the SE DCS's of Michelin *et al.* [19]. The good agreement between our calculated DCS's and experiments for energies above 50 eV, where the absorption effects are expected to be important, is particularly meaningful, and so it confirms the validity of the model potential used in the present study.

In Fig. 5 we compare our calculated ICS's and MTCS's in the (20–800)-eV range with the present measured results and also with some existing experimental data [9–11]. Our calculated and measured data agree with each other within the experimental uncertainties in the entire energy range in which the comparison is made. On the other hand, in general, the experimental ICS's and MTCS's of Marinković *et al.* [9] and Johnstone and Newell [11] lie significantly below our calculated data. Considering the good agreement between

our calculated and their measured DCS's, we suspect that the discrepancies may be due to the extrapolation procedure adopted by these authors.

In view of the substantial discrepancy between the calculated HF and experimental values of the dipole moment for this molecule, some test runs were made using the experimental value of D in Eqs. (16) and (17), in order to verify its influence on the calculated DCS's, mainly near the forward direction. It was found that the resulting discrepancy in the DCS's is lower than 4% at a scattering angle of $5°$ and an incident energy of 20 eV. This difference becomes much smaller for both larger scattering angles and higher energies. As a result, the discrepancies in the corresponding ICS's are about 4% at 20 eV and less than 1.5% at 100 eV and above.

Figures 6(a) and 6(b) show our calculated TCS's and TACS's, respectively, in comparison with some experimental data [5,16,54]. The TCS's of Joshipura and Patel [55] calculated using the additivity rule for energies above 100 eV are also shown for comparison. In general, the present calculated TCS's agree quite well with the experimental data in the entire energy range covered in this work. The calculated TCS's of Joshipura and Patel agree with our data at incident energies above 300 eV. Nevertheless, it is expected that the additivity rule approach does not work appropriately for incident energies below 100 eV, as can be inferred by the trend of their calculated TCS's towards lower incident energies. The comparison of our calculated TACS's and the experimental TICS's [16] shows very good qualitative agreement. Quantitatively, our results are systematically lower than experimental results and the discrepancy seen in Fig. 6(b) varies approximately from 10% to 30%. Considering that the ionization contribution to our TACS's is between 80% and 100% as stated before, we conclude that the present model potential underestimates the TACS's at most by 44%. In view of the simplicity of our model potential, this disagreement is still reasonable. However, further investigations in order to improve the calculated TACS's are needed.

Considering the scarceness of both theoretical and experimental cross sections for elastic electron scattering by this important gaseous molecule, it is hoped that the results reported in the present study can be useful for applications in plasma modeling and atmospheric studies. For that, our measured elastic DCS's, ICS's, and MTCS's are also shown in Table I.

In summary, we report a joint theoretical-experimental study on the elastic electron scattering by N_2O in the intermediate energy range. In general, our calculated and measured DCS's agree quite well with each other, and also agree well with some previous experimental data available in the literature. Also, the comparison of our calculated TCS's with available experimental results is encouraging. However, improvement on our absorption model potential is needed in order to yield more reliable TACS's.

[1] J. Hahn and C. Junge, Z. Naturforsch. A **32**, 190 (1977).

[2] W. Wang and N.D. Sze, Nature (London) **286**, 589 (1980).

[3] R.P. Wayne, Sci. Prog. **74**, 379 (1991).

[4] K.E. Fox and J. Reid, J. Opt. Soc. Am. B **2**, 807 (1985).

[5] C.K. Kwan, Y.-F. Hsieh, W.E. Kauppila, S.J. Smith, T.S. Stein, M.N. Uddin, and M.S. Dababneh, Phys. Rev. Lett. **52**, 1417 (1984).

[6] C. Szmytkowski, K. Maciag, and G. Karwasz, Chem. Phys. Lett. **107**, 481 (1984).

[7] C. Szmytkowski, K. Maciag, G. Karwasz, and D. Filipović, J. Phys. B **22**, 525 (1989).

[8] M. Kubo, D. Matsunaga, K. Koshio, T. Suzuki, and H. Tanaka, in *Collision Research in Japan*, edited by Y Hatano *et al.* (Society for Atomic Collision Research, Tokyo, 1981), Vol. 7, Progress Report 4.

[9] B. Marinković, Cz. Szmytkowski, V. Pejčev, D. Filipović, and L. Vuaković, J. Phys. B **19**, 2365 (1986).

[10] J.C. Nogueira, L. Mu-Tao, I. Iga, and M.A.E. Ferreira, J. Braz. Chem. Soc. **1**, 63 (1990).

[11] W.M. Johnstone and W.R. Newell, J. Phys. B **26**, 129 (1993).

[12] R. Azria, S.F. Wong, and G.J. Schulz, Phys. Rev. A **11**, 1309 (1975).

[13] M. Tronc, L. Malegat, R. Azria, and Y. Le Coat, in *Proceedings of the 12th International Conference on Physics of Electronic and Atomic Collisions*, edited by S. Dat (North-Holland, Amsterdam, 1981), p. 372.

[14] L. Andrić and R. Hall, J. Phys. B **17**, 2713 (1984).

[15] S.M. Barnett, N.J. Mason, and W.R. Newell, Chem. Phys. **153**, 283 (1991).

[16] I. Iga, M.V.V.S. Rao, and S.K. Srivastava, J. Geophys. Res., [Planets] **101**, 9261 (1996).

[17] M. Kitajima, Y. Sakamoto, S. Watanabe, T. Suzuki, T. Ishikawa, H. Tanaka, and M. Kimura, Chem. Phys. Lett. **309**, 414 (1999).

[18] M. Kitajima, Y. Sakamoto, R.J. Gulley, M. Hoshino, J.C. Gibson, H. Tanaka, and S.J. Buckman, J. Phys. B **33**, 1687 (2000).

[19] S.E. Michelin, T. Kroin, and M.-T. Lee, J. Phys. B **29**, 4319 (1996).

[20] K.B. Sarpal, K. Pfingst, B.M. Nestmann, and S.D. Peyerimhoff, J. Phys. B **29**, 857 (1996).

[21] S.M.S. da Costa and M.H.F. Bettega, Eur. Phys. J. D **3**, 67 (1998).

[22] L.A. Morgan, C.J. Gillan, J. Tennyson, and X. Chen, J. Phys. B **30**, 4087 (1997).

[23] C. Winstead and V. McKoy, Phys. Rev. A **57**, 3589 (1998).

[24] M.-T. Lee, I. Iga, L.E. Machado, and L.M. Brescansin, Phys. Rev. A **62**, 062710 (2000).

[25] G. Staszewska, D.W. Schwenke, and D.G. Truhlar, Phys. Rev. A **29**, 3078 (1984).

[26] R.R. Lucchese, G. Raseev, and V. McKoy, Phys. Rev. A **25**, 2572 (1982).

[27] A.W. Fliflet and V. McKoy, Phys. Rev. A **21**, 1863 (1980).

[28] M.-T. Lee and V. McKoy, Phys. Rev. A **28**, 697 (1983).

[29] M.-T. Lee, S. Michelin, L.E. Machado, and L.M. Brescansin, J. Phys. B **26**, L203 (1993).

[30] K.N. Joshipura, M. Vinodkumar, and U.M. Patel, J. Phys. B **34**, 509 (2001).

[31] N.T. Padial and D.W. Norcross, Phys. Rev. A **29**, 1742 (1984).

[32] J. O. Hirschfelder, C. F. Curtis, and R. B. Bird, *Molecular Theory of Gases and Liquids* (Wiley, New York, 1954).

[33] C. J. Joachain, *Quantum Collision Theory* (North-Holland, Amsterdam, 1983).

[34] T.H. Dunning, J. Chem. Phys. **55**, 716 (1971).

[35] J.M.L.J. Reinartz, W.L. Meerts, and A. Dymanus, Chem. Phys. **31**, 19 (1978).

[36] I. Iga and M.-T. Lee, J. Phys. B **32**, 453 (1999).

[37] I. Iga, M.-T. Lee, M.G.P. Homem, L.E. Machado, and L.M. Brescansin, Phys. Rev. A **61**, 022708 (2000).

[38] S.K. Srivastava, A. Chutjian, and S. Trajmar, J. Chem. Phys. **63**, 2659 (1975).

[39] R.T. Brinkman and S. Trajmar, J. Phys. E **14**, 245 (1981).

[40] M.A. Khakoo and S. Trajmar, Phys. Rev. A **34**, 138 (1986).

[41] J.C. Nickel, P.W. Zetner, G. Shen, and S. Trajmar, J. Phys. E **22**, 730 (1989).

[42] M.J. Brunger, S.J. Buckman, D.J. Newman, and D.T. Alle, J. Phys. B **24**, 1435 (1991).

[43] D.T. Alle, R.J. Gulley, S.J. Buckman, and M.J. Brunger, J. Phys. B **25**, 1533 (1992).

[44] S.J. Buckman, R.J. Gulley, M. Moghbelalhossein, and S.J. Bennett, Meas. Sci. Technol. **4**, 1143 (1993).

[45] M.A. Khakoo, T. Jayawera, S. Wang, and S. Trajmar, J. Phys. B **26**, 4845 (1993).

[46] H. Tanaka, T. Ishikawa, T. Masai, T. Sagara, L. Boesten, M. Takekawa, Y. Itikawa, and M. Kimura, Phys. Rev. A **57**, 1798 (1998).

[47] D.R. Olander and V. Kruger, J. Appl. Phys. **41**, 2769 (1970).

[48] A. Roth, *Vacuum Technology* (North-Holland, Amsterdam, 1982).

[49] *Handbook of Chemistry and Physics*, edited by D. V. Lide (CRC Press, Boca Raton, FL, 1993), Vol. 73.

[50] R.H.J. Jansen, F.J. de Heer, H.J. Luyken, B. van Wingerden, and H.J. Blaauw, J. Phys. B **9**, 185 (1976).

[51] R.D. Dubois and M.F. Rudd, J. Phys. B **9**, 2657 (1976).

[52] J.C. Nickel, C. Mott, I. Kanik, and D.C. McCollum, J. Phys. B **21**, 1867 (1988).

[53] L. Boesten and H. Tanaka, J. Phys. B **24**, 821 (1991).

[54] S. Xing, F. Zhang, L. Yao, C. Yu, and K. Xu, J. Phys. B **30**, 2867 (1997).

[55] K.N. Joshipura and P.M. Patel, Z. Phys. D: At., Mol. Clusters **29**, 269 (1994).